Advanced Composites and Hybrid Materials (2020) 3:485–497
https://doi.org/10.1007/s42114-020-00178-w

ORIGINAL RESEARCH

Preparation, characterization, and antimicrobial activity of chitosan/gum arabic/polyethylene glycol composite films incorporated with black pepper essential oil and ginger essential oil as potential packaging and wound dressing materials

Augustine Amalraj[1,2] · K. K. Jithin Raj[1] · Józef T. Haponiuk[2] · Sabu Thomas[3] · Sreeraj Gopi[1,2]

Received: 4 February 2020 / Revised: 21 August 2020 / Accepted: 10 September 2020 / Published online: 29 September 2020

Abstract

Essential oils (EOs), black pepper essential oil (BPEO), and ginger essential oil (GEO) exhibit excellent antimicrobial, antioxidant, nutritional, and biomedical properties; however, poor aqueous solubility and instability of their constituents reduced the retention of these properties for the longer time. In this study, biocomposite films based on the chitosan- (CS), gum arabic– (GA), and polyethylene glycol (PEG)–incorporated BPEO and GEO were fabricated by solvent casting method to overcome the limitations and the sensitivity of the EOs. The interaction of the EOs with composite matrix was evaluated using Fourier transform infrared (FTIR) spectroscopy, X-ray diffraction (XRD), scanning electron microscopy (SEM), and differential scanning calorimetry (DSC) were performed with the determination of swelling degree, water solubility, volatile mass fraction, and mechanical properties. The BPEO-CS/GA/PEG film showed rough surface with coarseness nature due to the migration of BPEO towards CS/GA/PEG surface; likewise, GEO-CS/GA/PEG appeared rough surface whereas showed more cavities with entrapment of GEO droplets. The BPEO- and GEO-incorporated CS/GA/PEG films showed great mechanical strength and flexibility with high thermal stability. The BPEO- and GEO-incorporated CS/GA/PEG films showed high antimicrobial activity against *Bacillus cereus*, *Staphylococcus aureus*, *Escherichia coli*, and *Salmonella typhimurium.* The obtained results have demonstrated that both BPEO- and GEO-incorporated CS/GA/PEG films are promising alternatives to food packaging and wound dressing materials.

Keywords Black pepper essential oil · Ginger essential oil · Chitosan/gum arabic/poly ethylene glycol composite film

1 Introduction

Essential oils (EOs) are compounds extracted from aromatic plants, which are the mixture of volatile compounds including terpenes, esters, phenols, and aromatic hydrocarbons [1, 2]. The EOs are used in various applications in pharmaceutical, medicinal, nutraceutical, cosmaceutical, and food industries due to their antioxidant, anti-inflammatory, antibacterial, antifungal, sedative, analgesic, spasmolytic, and flavoring properties [3], even though the utilization of EOs is limited due to its water insolubility, low stability, characteristic taste, which alter the sensory properties, because most of the ingredients of EOs can be easily oxidized and deteriorated when exposed to the light, heat, and environment oxygen [1, 2].

Encapsulation technology provided an effective approach to incorporate the EOs with high stability with a bioavailable form by the prevention of loss of their active volatile ingredients [2]. The incorporation of EOs in the composite films has been in recent times accepted technique to keep aroma components from destructive changes, particularly in food packaging and wound dressing materials. Active food packaging is a fast developing and auspicious technology in which the

✉ Sreeraj Gopi
sreeraj.gopi@plantlipids.com

[1] R&D Centre, Aurea Biolabs (P) Ltd, Kolenchery, Cochin, Kerala 682 311, India

[2] Chemical Faculty, Gdansk University of Technology, Gdańsk, Poland

[3] International and Inter University Centre for Nanoscience and Nanotechnology, School of Chemical Sciences, Mahatma Gandhi University, Priyadarshini Hills P. O., Kottayam, Kerala 686 560, India

antimicrobial or antioxidant agents are incorporated into the packaging materials. It can provide the packed food high quality, safety, and long shelf life, usually by dropping or hindering the development of microorganisms. Wound dressings are used to stop bleeding, guard wound against infections, absorb excess exudates, and uphold wound hydration to quicken the healing process by the incorporation of bioactive components. Recently, the production of EO-incorporated composite films is a rising attention to fabricate an innovative generation of wound dressings and food packaging materials composed of different varieties of natural or synthetic or their combinations with suitable biological characteristics [4–9].

In recent years, the incorporation of bioactive compounds using natural biopolymers has concerned significant interest. They exhibit enhanced stability, bioavailability, and bioefficacy, improved aqueous solubility of lipophilic compounds, excellent biodegradability, and reduced toxicity [10–14]. Among the biopolymers, chitosan (CS) and gum arabic (GA) have been widely used as encapsulating material owing to their biocompatibility, low toxicity, etc. CS is the second most plentiful polysaccharide and a product of the deacetylated chitin, which has been widely applied in various fields, especially in biomedical, pharmaceutical, nutraceutical, and functional foods. Moreover, CS is considered as promising positively charged polysaccharide for preparing composite films owing to its good film-forming ability, biocompatibility, and biodegradation with bio-adhesive and antimicrobial properties [13]. Numerous studies have reported that CS films had enhanced antimicrobial activities with high water resistance during the encapsulation of EOs [13–16] due to the interactions with the majority of the aromatic compounds by hydrogen bonding [17] and through the Schiff-based reactions [18]. However, there are some limitations for CS to be applied because of its solubility in aqueous acidic solution below pH 6.5, while insoluble in neutral pH and physiological environment [19]. Furthermore, the EO-encapsulated CS films did not exhibit improvement in retention and release properties of EOs due to the weak hydrogen bonding between CS and EOs, which was not enough for the retention of volatile compounds in EOs [20, 21]. In order to overcome these drawbacks, the addition of other encapsulating agents such as the addition of emulsifier or polymers into the CS matrix could improve the compatibility of the multi-phased system, thus enhanced the retention and release properties of EOs [22]. GA is a negatively charged polysaccharide-protein complex with admirable emulsifying properties, which is obtained from the stems and branches of acacia trees. The hydrophilic parts facilitate stabilizing the emulsion against droplet aggregation, while the hydrophobic branched proteins are quickly adsorbed onto the emulsion droplet surface [23, 24]. GA had unique characteristics such as commercial availability, high solubility, less viscosity, emulsification, good film forming, non-toxic, and biocompatibility [25, 26]. GA could overcome the stability, solubility, and bioavailability issues of antioxidants due to the presence of amino acids [26]. Furthermore, to assist CS composite film formation, usage of polyethylene glycol (PEG) is quite common as a biodegradable, biocompatible, non-toxic, and water-soluble synthetic polymer composed of repeating ethylene glycol units, which is approved by FDA for various biomedical applications [27]. The PEG is a polymer that is well known for its smooth film-forming capacity, easy process ability, and chemical resistance properties, which is effectively utilized in nutraceutical, pharmaceutical, and medical fields [19, 28].

Ginger (*Zingiber officinale* Roscoe) and black pepper (*Piper nigrum* L.) are linked with numerous health benefits which have led to their broad use in a variety of commercial natural products offered in the emerging nutraceutical and functional foods market due to their various biological properties such as antimicrobial, antioxidant, anti-inflammatory, anticancer, and antidiabetic activities [10, 29]. Ginger essential oil (GEO) is extracted from the roots of the plant *Zingiber officinale* Roscoe. The main chemical compounds of GEO are α-zingiberene, β-sesquiphellandrene, camphene, and ar-curcumene [11, 30]. Black pepper essential oil (BPEO) is basically composed of terpenes, which have been found to be β-caryophyllene, pinene, δ-3-carene, and limonene [29, 31]. Both GEO and BPEO are widely used EOs worldwide, and have been reported to possess strong antimicrobial, antifungal, and antioxidant activities [11, 29].

In this study, the selection of GEO and BPEO was mainly based on their well-established biomedical activities and phytochemical components. The aim of the study is the incorporation of GEO and BPEO in CS/GA/PEG composite film by solvent casting technique to enhance the stability of EOs, protect their bioactive constituents, attain sustained release profile, and improve their antibacterial activities for food, nutraceutical, pharmaceutical, and bio-medicinal applications due to the advancement of antimicrobial activity, healing property compared with traditional packing and dressings. The incorporation of EOs was investigated using different characterization techniques, viz. IR, XRD, DSC, and SEM along with the physical, thermal, and mechanical properties. In addition, retention and release studies were estimated for both incorporated EOs. Furthermore, the antibacterial activity was also studied for incorporated EOs.

2 Experimental

2.1 Materials

Black pepper essential oil and ginger essential oil were obtained from Plant Lipids Private Limited, Cochin, Kerala, India. Gum arabic was obtained from Cargill India Pvt. Ltd., Gurgaon, India. Ninety percent deacetylated chitosan (80

meshes) was purchased from Pelican Biotech Chemicals and Laboratory, Kerala, India. Polyethylene glycol (Mw = 4000 g/mol) and all other chemicals were purchased from Merck India, Mumbai, India. Millipore-MilliQ distilled water was used during the complete study.

2.2 Composition of BPEO and GEO

The BPEO and GEO compositions were analyzed by a gas chromatograph coupled with mass spectrometer using Bruker 436-GC, couple with SCION TQMS by Rtx-624 fused silica column with 60 m column length and 0.25 mm internal diameter. The temperature was held at 90 °C for 5 min and then programmed to first column temperature ramp of 150 °C at a rate of 8 °C/min, retained for 10 min and programmed to second column temperature ramp of 210 °C at a rate of 5 °C/min for 8 min and raised to the final temperature 230 °C at a rate of 10 °C/min and kept constant for 15 min. The injector and detector temperature were adjusted to 225 °C and 240 °C, respectively. Helium gas was used as the carrier gas at 1 mL/min of flow rate with constant pressure as 228 kPa. The results of the GC have interpreted using National Institute of Standard Technology – MS search library version 2.0 (NIST 14).

2.3 Preparation of CS/GA/PEG composite film with and without BPEO and GEO

The CS was dissolved in the acetic acid at room temperature to prepare 2% (w/v) CS solution. The 50% (w/v) of GA was prepared by dissolving GA in MilliQ Millipore water at 50 °C. Then, the PEG solution 17% (w/v) was prepared by dissolving PEG in MilliQ Millipore water at 80 °C under constant mechanical stirring for 6 h. After that, the blend CS/GA/PEG solution was prepared by mixing the CS, GA, and PEG solution and which was stirred constantly using a mechanical stirrer for 15 min. Then, glycerol (1 g) was added and the resulting mixture, CS/GA/PEG composite, became viscous and was homogenized under mechanical stirring for 30 min at 80 °C. Then, the BPEO or GEO was added in different percentage (10, 15, 20, 25, 30, 40, and 50) into the CS/GA/PEG composite solution under stirring for 15 min and the mixed solutions were homogenized under high pressure in a PRIMIX-Homomixer Mark II.2.5 homogenizer with a pressure range of 30–300 bar and the process was repeated three times. Based on the homogenization ability, 10% of BPEO as well as GEO was fixed to make BPEO- and GEO-incorporated CS/GA/PEG composite films. Then, these film-forming solutions were degassed in the vacuum drying oven (Rotek Vaccum Oven). The films were prepared by solution casting method and the mixed solutions onto the acrylic plates at 60 °C. The films were dried for 40 min at 50 °C and then peeled from the caster plates. The prepared BPEO- and GEO-incorporated composite films were marked as BPEO-CS/GA/PEG and GEO- CS/GA/PEG, respectively, as well as a control film was also prepared and marked as CS/GA/PEG which were preserved under relative humidity 50% at a temperature of about 25 °C for the additional analysis. A schematic illustration representing the preparation of CS/GA/PEG composite film with and without BPEO and GEO is shown in Fig. 1.

2.4 Characterization of prepared BPEO- and GEO-incorporated CS/GA/PEG composite films

2.4.1 Swelling degree and water solubility

The swelling degree and water solubility were calculated according to Akyuz et al. [32] with suitable modifications. The dried pieces of composite film (W_1) were placed in 50-mL beakers with 30 mL of distilled water covered by plastic wraps, which were shaken in a thermostatic shaker at a speed of 30 rpm for gentle agitation at room temperature (28 ± 2 °C). After 24 h, the swollen films were taken out of the water and gently blotted with filter paper, weighted accurately (W_2); the equation below was used to calculate the percentage of moisture gained.

$$\text{Swelling degree}\ (\%) = \frac{(W_2 - W_1)}{W_1} \times 100 \quad (1)$$

where W_1 and W_2 are the weight of the dried and swollen films (g), respectively.

Consequently, the swollen film pieces were dried at 50 °C for 24 h and reweighed. The percentage of dissolved dry content in water was calculated by the following equation:

$$\text{Water solubility}\ (\%) = \frac{(W_1 - W_3)}{W_1} \times 100 \quad (2)$$

where W_3 is the final weight (g) after drying.

2.4.2 Volatile mass fraction

Approximately 25 mm × 25 mm of samples cut from the films and weighted before (W_a) and after (W_b) drying in an oven at 105 °C for 24 h to calculate the volatile mass fraction using the following equation:

$$\text{Volatile mass fraction}\ (\%) = \frac{(W_a - W_b)}{W_a} \times 100 \quad (3)$$

2.4.3 Thickness and mechanical properties

The thickness of the films was determined using the arithmetic mean of five random measurements of their surface, including the center, the surroundings, and the remaining random

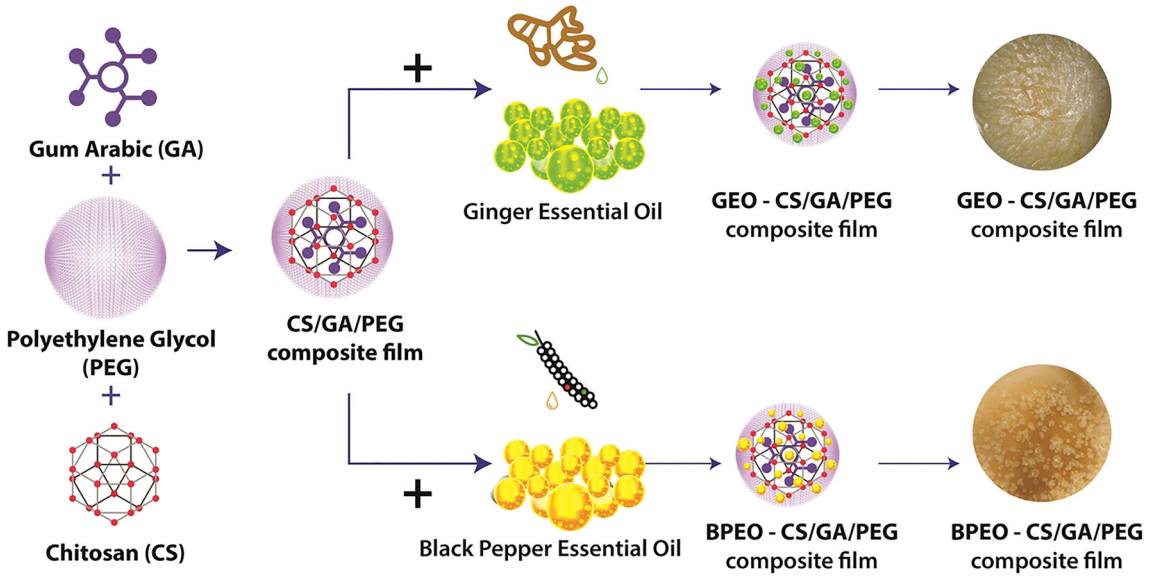

Fig. 1 Schematic illustration of the preparation of CS/GA/PEG composite film with and without BPEO and GEO

positions by using a digital thickness gauge (Mitutoyo model) and the results were expressed in mm.

The mechanical properties (tensile strength and elongation) of the films were determined with the help of H50KT (Tinius Olsen), a universal testing machine, according to the ATM D 882 method, ASTM, 1995 [33]. The experiments were carried out at a cross speed of 10 mm/min maintaining a room temperature of 27 ± 3 °C. The dimension of the samples was 50 mm × 10 mm and the results were the average of five measurements.

2.4.4 Fourier transform infrared-attenuated total reflectance spectroscopy

The Fourier transform infrared-attenuated total reflectance (FTIR-ATR) spectra recorded by JASCO ATR-FT/IR-4700 for CS/GA/PEG and BPEO- and GEO-incorporated CS/GA/PEG composite films were in the range of 400–4000 cm^{-1} with 32 scans per samples.

2.4.5 X-ray diffraction

The crystalline nature of the CS/GA/PEG and BPEO- and GEO-incorporated CS/GA/PEG composite films were determined using X-ray diffraction pattern analysis (X'pert3 powder X-ray Diffractometer, UK) at ambient temperature using CuKα radiation ($\lambda = 1.5406$ nm) over the 2θ range of 10 and 90° with a scanning speed of 1.2 °/min. The prepared composite films were vacuum dried at 60 °C before the assay.

2.4.6 Scanning electron microscopy

Scanning electron microscope (Vega3Tescan, Czech Republic) was employed to investigate the surface morphology of CS/GA/PEG and BPEO- and GEO-incorporated CS/GA/PEG composite films. The prepared films were placed in aluminum stubs using double-sided carbon tape and sputter coated with gold. An accelerating voltage of 20–30 kV was used to scan the prepared composite films.

2.4.7 Differential scanning calorimetry

The thermal property of prepared CS/GA/PEG and BPEO- and GEO-incorporated CS/GA/PEG composite films was estimated with differential scanning calorimeter (DSC) Q10 DSC equipment (Mettler Tolcdo DSC822e, India). All the film samples were dried for 1 week in a desiccator over P_2O_5 before analysis. Approximately 5 mg of each film was cut into small portions and placed on a small pan. The reference was an empty pan. The samples were heated from 25 to 300 °C under a nitrogen atmosphere, then cooling to 25 °C and a second heating to 300 °C with a heating and cooling rate of 10 °C/min.

2.5 Retention and release study

2.5.1 The retention of BPEO and GEO during ambient storage

The retention of BPEO and GEO during the film storage (25 °C, 50% relative humidity) was quantified by the method of Xu et al. [13] with suitable modifications. Both BPEO- and GEO-incorporated CS/GA/PEG composite films 1 g of each

were separately placed in a centrifuge tube with 30 mL of hexane was added and vigorously stirred overnight at 25 °C. The solution was centrifuged at 10,000 rpm for 15 min and then the supernatant was measured by an ultraviolet spectrophotometer (Perkin Elmer Lambda 35) with the absorbance at 310 nm for BPEO and 340 nm for GEO, which were calibrated by a standard curve obtained from standard BPEO and GEO solutions in hexane. The loss of BPEO and GEO was calculated as the ratio of decreased amounts of BPEO and GEO in the films to the original amount of BPEO and GEO in the film-forming solution. The measurements were taken once a day for a total of 14 days. Each sample was performed for five repetitions.

2.5.2 BPEO and GEO release profile

In order to establish the release rate of the BPEO- and GEO-incorporated CS/GA/PEG composite films, 60% glycerol was chosen as a simulating solution for various applications, particularly for food packaging and wound healing activities. The BPEO and GEO release towards simulant were quantified with the method modified from Xu et al. [13]. Both BPEO- and GEO-incorporated CS/GA/PEG composite films 1 g were cut into equal parts and immersed in 30 mL simulating solution with constant stirring at 50 rpm. Then, 1 mL solution was pipetted at regular intervals and dissolved in hexane to be measured the absorbance by the ultraviolet spectrophotometer at 310 nm for BPEO and 340 nm for GEO. All measurements were replicated five times.

2.6 Antimicrobial activity

The antimicrobial activity of the films was evaluated using disc diffusion method [34] against four bacterial species, which are *Bacillus cereus* (*B. cereus*), *Staphylococcus aureus* (*S. aureus*), *Escherichia coli* (*E. coli*), and *Salmonella typhimurium* (*S. typhimurium*). Films (1 g) were initially immersed in 20-mL nutrient broth for 1 h to swell. The bacteria were preserved in the Müeller-Hinton agar (MH). Inocula were prearranged with accumulation and during the night civilization of the organism in MH broth to obtain an OD_{600}.0.1. The cells were permitted to cultivate and attain the McFarland standard 0.5, i.e., approximately 10^8 CFU/mL. The suspensions were diluted to 1:1000 in MH broth to attain 10^6 CFU/mL. The conditioned film discs were positioned directly on Mueller-Hinton agar plates with the earlier wiped objective bacterial segregate at a concentration of 10^6 CFU/mL. The petri plates were then incubated overnight at an incubation temperature of 37 °C. The antimicrobial activity was evaluated by measuring the zone of inhibition against the tested microorganism.

2.7 Statistical analysis

The experiment determinations were completed in five replicates and the average values, mean, and standard deviation are reported. Statistical comparisons were made by using one-way ANOVA followed by Duncan's multiple range test by using SPSS 16.0 and the OriginPro 8.5 statistics program. Differences were observed as significant at 95% ($p < 0.05$).

3 Results and discussion

3.1 Essential oil composition of black pepper and ginger

The BPEO that showed the presence of 31 major compounds is shown in Table 1, which was caryophyllene (28.96%), followed by 3-carene (6.86%), D-limonene (6.25%), β-pinene (3.15%), β-selinene (3.01%), δ-elemene (2.95%), D-α-Pinene (2.88%), α-Copaene (2.73), Caryophyllene oxide (2.37%), α-Selinene (2.06%), and humulene (1.99%). The availability of other constituents was lower than 2%. These results are in good agreement with the findings of Rouatbi et al. [35] and Myszka et al. [36], who reported that caryophyllene, careen, and limonene are the main constituents of BPEO. However, there are few differences in main chemical compounds of BPEO were reported some studies [37, 38] may be due to the genetic, age and stage of maturity, weather conditions, soil composition, plant organs, distillation conditions, and some other factors.

The GEO presented 40 major components (Table 1), and the main constituents were α-zingiberene (28.85%), β-cedrene (20.21%), α-curcumene (14.23%), β-bisbolene (11.294%), β-sesquiphellandrene (8.39%), E-β-Famesene (2.89%), and β-panasinsene (2.43%). The presence of other constituents was lower than 2%. Silva et al. [1] and Noori et al. [11] evaluated GEO and reported comparable composition, with α-zingiberene being the main organic constituent. Variations in the composition of GEO from *Zingiber officinale* Roscoe may be due to genetic, plant age, environmental composition, and different extraction process. The compositions of both EOs, BPEO and GEO, directly influence their biological activities as each compound has a specific ability.

3.2 Characterization of prepared CS/GA/PEG composite films with and without BPEO and GEO

3.2.1 Swelling degree

The swelling degree of the films is given in Table 2. According to the results, the CS/GA/PEG composite film confirmed a high degree of swelling, and this may be due to the hydrophilic nature of CS [13] and GA [34] which enhance the

Table 1 Compositions of black pepper and ginger essential oils

Black pepper essential oil			Ginger essential oil		
Compound	Retention time (min)	Concentration (%)	Compound	Retention time (min)	Concentration (%)
α-Thujene	13.24	0.33	α-pinene	13.76	0.53
D-α-Pinene	13.77	2.88	Camphene	14.66	1.48
L-β-Pinene	15.37	0.43	D-Limonene	17.90	0.35
β-Terpinene	15.45	2.32	β-Phellandrene	18.38	1.36
β-Pinene	15.87	3.15	Fa-Eucalyptol	18.72	1.11
α-Phellandrene	16.75	1.16	β-Linalool	22.35	0.16
3-Carene	16.96	6.86	Terpinen-4-ol	26.65	0.15
D-Limonene	17.91	6.25	endo-Borneol	27.14	0.45
p-Cymene	18.14	0.47	L-α-Terpineol	27.47	0.66
β-Phellandrene	18.40	0.37	Citronellol	28.28	0.38
γ-Terpinene	19.25	0.10	Geraniol	29.43	0.52
Terpinolene	20.82	0.39	Cis-Verbenol	29.79	0.29
β-Linalool	22.37	0.32	Citral	30.88	0.47
Terpinen-4-ol	26.67	0.11	α-Cubebene	32.16	0.16
δ-Elemene	31.71	2.95	Citronellyl isobutyrate	32.28	0.11
α-Copaene	33.75	2.73	Geranyl acetate	33.60	0.63
β-Elemene	34.52	1.57	α-Copaene	33.73	0.38
α-Gurjunene	35.57	0.24	E-β-Famesene	34.50	2.89
Piperonal	35.84	0.12	α-Bergamotene	35.93	0.25
α-Guaiene	36.62	0.39	Cis-β-Farnescene	36.15	0.47
Caryophyllene	36.81	28.96	γ-Elemene	36.19	0.56
Humulene	38.62	1.99	β-Copaene	36.80	0.42
Guaia-1(10),11-diene	39.79	0.22	Chamigrene	37.99	0.19
β-Selinene	40.04	3.01	β-Himachalene	38.16	1.48
α-Selinene	40.21	2.06	α-Curcumene	38.65	14.23
δ-Cadinene	40.50	1.39	α-Zingiberene	38.85	28.85
α-Copaene	41.33	0.27	β-Bisbolene	39.43	11.29
(-)-Spathulenol	46.16	0.20	Isoledene	39.61	0.58
Caryophyllene oxide	46.68	2.37	α-Muurolene	39.67	0.51
Spathulenol	48.77	1.19	Eremophilene	40.05	0.56
τ-Cadinol	49.04	0.16	β-Panasinsene	40.35	2.43
			β-Cedrene	40.50	20.21
			β-Cubebene	40.95	0.32
			β-Sesquiphellandrene	41.20	8.39
			α-Panasinsen	41.35	1.21
			E-Nerolidol	42.70	1.25
			Elemol	43.91	1.27
			Verticiol	47.89	1.92
			β-bisabolan	49.91	0.32
			β-Selineol	50.65	0.91

water uptake ability. The incorporation of both EOs, BPEO and GEO, significantly ($p < 0.05$) decreased the swelling degree of the EO-incorporated films due to the higher level of the hydrophobic nature of the BPEO and GEO. Furthermore, the fact that the BPEO and GEO are able to decrease the tendency of the CS/GA/PEG composite film matrix to bind water and thus reduce the water uptake, along with which reduced the number of available groups in the network that

Table 2 Properties of CS/GA/PEG composite films with and without BPEO and GEO

Composite film	Swelling degree (%)	Water solubility (%)	Volatile mass fraction (%)	Thickness (mm)	Tensile strength (MPa)	Elongation (%)
CS/GA/PEG	184.74 ± 8.76	58.24 ± 5.36	19.42 ± 3.63	1.93 ± 1.04	10.14 ± 1.24	68.94 ± 7.12
BPEO-CS/GA/PEG	143.89 ± 8.04*	46.44 ± 3.74*	15.74 ± 3.42*	2.84 ± 1.12*	5.67 ± 1.32*	72.66 ± 6.34*
GEO-CS/GA/PEG	138.32 ± 7.41*	39.71 ± 4.38*	12.84 ± 2.14*	2.19 ± 1.32*	7.58 ± 1.73*	79.46 ± 6.19*

Values are mean ± SD of five replicates

Significant difference exists at $*p < 0.05$

were capable of hydrogen bond formation with water molecules, thereby reducing the swelling degree [14]. Likewise, flaxseed oil–incorporated soy protein–based films [39] and *Zataria multiflora* EO-incorporated polyvinyl alcohol–based electrospun [5] reduced the swelling degree probably due to the reduction of interaction between water and film matrix.

3.2.2 Water solubility

Water solubility is a main factor for various applications of the film, particularly packaging and wound dressing materials. The water solubility can be considered an indicator to evaluate the stability of the films and water resistance, because the solubility of the films depends the type and concentration of the components as well as their hydrophilicity and hydrophobicity indices. Consequently, hydrophilic components tend to increase the solubility values, whereas hydrophobic components decrease the solubility [40, 41].

The solubility of the BPEO and GEO with and without CS/GA/PEG composite films in distilled water at room temperature was investigated as a percentage, as given in Table 2. The prepared CS/GA/PEG composite film was found to have higher water solubility (58.24%) when compared with BPEO- (46.44%) and GEO- (39.71%) incorporated CS/GA/PEG composite films due to the fact that both BPEO and GEO reacted effectively with the CS/GA/PEG composite matrix; it was tough to the entry of water molecules within the CS/GA/PEG composite matrix; moreover, the number of hydrophilic groups was reduced. Furthermore, EOs could function to possibly emulsify the polymeric matrix via a filling effect and the results in a compact and continuous structure of BPEO- and GEO-incorporated CS/GA/PEG composite film. In summary, more hydrophobic components in both BPEO and GEO were found (Table 1) to result in the destruction of hydrogen bonding between the CS, GA, and PEG in the CS/GA/PEG composite film and were found to interfere with the water attack, while were beneficial for producing integrity water proofing and their interactions may limit the hydrogen groups to form hydrophilic bonds with water and thus lead to a decrease in water affinity of the film.

3.2.3 Volatile mass fraction

Volatile mass fraction denotes to the percentage of film mass reduction in the initial weight of the film, as given in Table 2. The moisture content was the primary volatile component in the CS/GA/PEG composite film, which contained 19.42%. Conversely, the content of volatile matters in both BPEO- and GEO-incorporated CS/GA/PEG composite films containing not only moisture but also the EOs was 15.74% and 12.84% for BPEO-CS/GA/PEG and GEO-CS/GA/PEG composite films, respectively, which were lowered than the CS/GA/PEG composite film due to the strong interaction between the EOs and film matrix, which reduced the free volume in the film matrix, resulting in a slump in the film capacity for holding and capturing moisture. Therefore, the amount of moisture volatilized above 100 °C was decreased, which ultimately led to the volatile content of BPEO- and GEO-incorporated CS/GA/PEG composite films lower than that of CS/GA/PEG composite film. These results indicated the well incorporation of EOs onto the CS/GA/PEG composite films, which were similar to those described by Li et al. [14] and Sahraee et al. [42].

3.2.4 Thickness and mechanical properties

The incorporation of BPEO and GEO into the CS/GA/PEG composite film increased the thickness (2.89 mm and 2.19 mm, respectively), when compared with CS/GA/PEG composite film (1.93 mm) (Table 2) due to the entrapment of BPEO and GEO micro droplets into the CS/GA/PEG composite matrix, thereby increase the compactness of the CS/GA/PEG matrix structure. Similar results were reported with the addition of licorice EO onto carboxymethyl xylan film [43] and corn starch containing orange EO [41].

Mechanical properties of the films particularly the tensile strength and elongation are the important indicators of the applicability of films. Hypothetically, incorporation of EO is anticipated to interrupt polymeric network in the film, which would then result in a decrease in tensile strength and an increase in flexibility [44]. The mechanical properties of CS/GA/PEG and both BPEO- and GEO-incorporated CS/GA/PEG composite films are given in Table 2. Both BPEO- and

GEO-incorporated films showed slightly lower tensile strength values 5.67 ± 1.32 MPa and 7.58 ± 1.73 MPa, respectively, compared with CS/GA/PEG composite film (10.14 ± 1.24), might be the phase separation and migration of the components of the EOs in the composite matrix, which indicates to the fact that the incorporation of BPEO and GEO in the CS/GA/PEG composite film faintly weakened polymeric network [45]. Furthermore, stronger intermolecular interaction of CS/GA/PEG composite film can be partially replaced by the EO interactions generating more flexibility within the CS/GA/PEG composite film. On the other hand, elongation increased with the incorporation of BPEO and GEO onto the CS/GA/PEG composite film due to their plasticizing effects. Moreover, the mechanical properties of the films are affected by various factors, such as nature and structure of the polymers used, and the nature and content of EO and their droplet size and their distribution [39, 45].

3.2.5 Fourier transform infrared-attenuated total reflectance spectroscopy studies

The FTIR spectra of BPEO, GEO, and CS/GA/PEG composite films with and without BPEO and GEO are shown in Fig. 2A. The FTIR spectrum of BPEO (Fig. 2A (a)) consisted of the prominent absorption bands at 2957 cm^{-1}, 2918 cm^{-1}, and 2870 cm^{-1} for C–H stretching vibration of methylene group, 1653 cm^{-1} for H–O–H bending, 1437 cm^{-1} for C–H scissoring vibration, 1382 cm^{-1} and 1365 cm^{-1} for symmetrical deformation vibration of CH_3, 863 cm^{-1} for C–H deformation vibration, and 786 cm^{-1} for S–C absorption [29]. The absorption bands of GEO (Fig. 2A (b)) at 1621 cm^{-1} and 1593 cm^{-1} were associated with C=C stretching and the bands at 1462 cm^{-1} and 1339 cm^{-1} for stretching vibration of C=C–C=C. A vibration mode associated with $–CH_2$ groups is presented in the GEO at 2879 cm^{-1} and C–H bond stretching at 839 cm^{-1}. Furthermore, the C=O stretching is present with strong intensity at 1097 cm^{-1} [1, 46].

The FTIR spectrum of CS/GA/PEG composite film (Fig. 2A (c)) demonstrates peak at 3269 cm^{-1} which is attributed to N–H and O–H stretching vibration [5]. A band at 2933 cm^{-1} is related at C–H stretching, which is associated with the out of phase stretching of $R–CH_2–R$ [34]. The peaks at 2882 cm^{-1} and 1108 cm^{-1} indicated the $–CH_2$ groups and C–O–C stretching of PEG [47]. Another peak at 1633 cm^{-1} is associated with amino characterization. Two small bands at 1561 cm^{-1} and 1536 cm^{-1} in amide region are attributed to the N–H vibration [48]. A strong peak at 1412 cm^{-1} was derived from the symmetrical stretching vibration of the C=O group and characteristic –OH in plane bending vibrations in CHOH [34, 47, 49]. The peak at 1342 cm^{-1} is assigned to C–H bending vibration [5]. The bands at 1029 cm^{-1} and 923 cm^{-1}, and 844 cm^{-1} correspond to the C–O, C–C, and C–O–C stretching and C–O–H and C–H bending modes [5, 34]. Therefore, the prepared composite film is composed of all CS, GA, and PEG components.

On the other hand, the FTIR spectra of CS/GA/PEG composite films incorporated with BPEO and GEO were evaluated to specify the BPEO and GEO incorporation in the composite film structure. Based on the obtained results for the BPEO-incorporated CS/GA/PEG composite film (Fig. 2A (d)), it can be seen that beside the peaks at 3303 cm^{-1}, 2923 cm^{-1}, 2882 cm^{-1}, 1616 cm^{-1}, 1328 cm^{-1}, 1022 cm^{-1}, and 841 cm^{-1}, which manifest the presence of CS, GA, and PEG in the composite film, two new peaks at 1328 cm^{-1} and 770 cm^{-1} appeared which are attributed to typical bands of BPEO confirm the incorporation of BPEO into the CS/GA/PEG composite film [29]. The IR spectrum of GEO-incorporated CS/GA/PEG composite film (Fig. 2A (e)) demonstrates peaks at 3300 cm^{-1}, 2882 cm^{-1}, 1602 cm^{-1}, 1105 cm^{-1}, 1031 cm^{-1}, 961 cm^{-1}, and 841 cm^{-1}, which noticeable the presence of CS, GA, and PEG, whereas other new

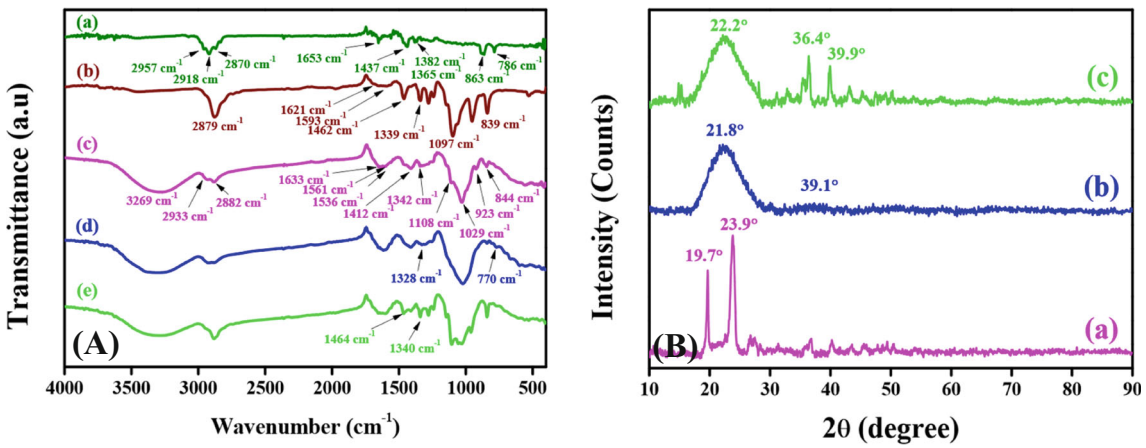

Fig. 2 (A) FTIR spectra of (a) BPEO, (b) GEO, (c) CS/GA/PEG, (d) BPEO-CS/GA/PEG, and (e) GEO-CS/GA/PEG composite films and (B) XRD diffraction pattern of (a) CS/GA/PEG, (b) BPEO-CS/GA/PEG, and (c) GEO-CS/GA/PEG composite films

peaks that appear at 1464 cm^{-1} and 1340 cm^{-1} indicate the incorporation of GEO onto the CS/GA/PEG composite film [1, 46].

3.2.6 X-ray diffraction studies

XRD analysis of CS/GA/PEG, BPEO-CS/GA/PEG, and GEO-CS/GA/PEG are presented in Fig. 2B. The XRD pattern of CS/GA/PEG film showed the characteristic peaks of mixture of the CS, GA, and PEG at 19.7° and 23.9° (Fig. 2B (a)), signifying the amorphous nature with significant crystallinity of CS, GA, and PEG. After incorporation of BPEO (Fig. 2B (b)) and GEO (Fig. 2C (c)) into CS/GA/PEG composite films, the peaks at 21.8° and 22.2° became broader and less intense, indicating the disruption of CS/GA/PEG composite film structure [12, 50]. Furthermore, a new peak at 39.1° in the XRD spectrum of the BPEO-CS/GA/PEG and two new peaks at 36.4° and 39.9° in the XRD pattern of the GEO-CS/GA/PEG nanocomposite films appeared, which are attributed to the incorporation of BPEO and GEO into the CS/GA/PEG composite film, respectively.

3.2.7 Scanning electron microscopy studies

The scanning electron micrographs of the surface of the BPEO and GEO incorporated and without the EO incorporation of CS/GA/PEG nanocomposite films are shown in Fig. 3 with different magnifications. The SEM micrographs of CS/GA/PEG composite films are shown in Fig. 3 (a) and Fig. 3 (b) in different magnifications as 100 μm and 20 μm, respectively, which exhibited compact, uniform, and smooth microstructure with cavities, which reflects the good compatibility and structural integrity of the three polymers of CS, GA, and PEG. However, the SEM micrographs of BPEO-CS/GA/PEG film are shown in Fig. 3 (c) and Fig. 3 (d) at the magnifications of 100 μm and 20 μm, respectively. As can be observed, the surface of the film containing BPEO was rougher than that of the CS/GA/PEG and also increased the coarseness of the film surface due to the migration of oil droplets towards the film surface and further volatilization of BPEO. The volatilization of the BPEO in addition to the evaporation of water resulted into irregular surface, which suggested the structural rearrangement of CS, GA, and PEG in the film matrix in the presence of BPEO. Similar results were reported in earlier studies, when the incorporation of EOs in different edible films increased the coarseness of the films [45, 51]. Likewise, the GEO-CS/GA/PEG composite film (Fig. 3 (e and f)) showed a hetero-structure in which GEO droplets are trapped in the CS/GA/PEG network with increased roughness and the appearance of more cavities without cracks due to the hydrophobicity of the GEO in the CS/GA/PEG composite film and revealing incorporation of the GEO in the CS/GA/

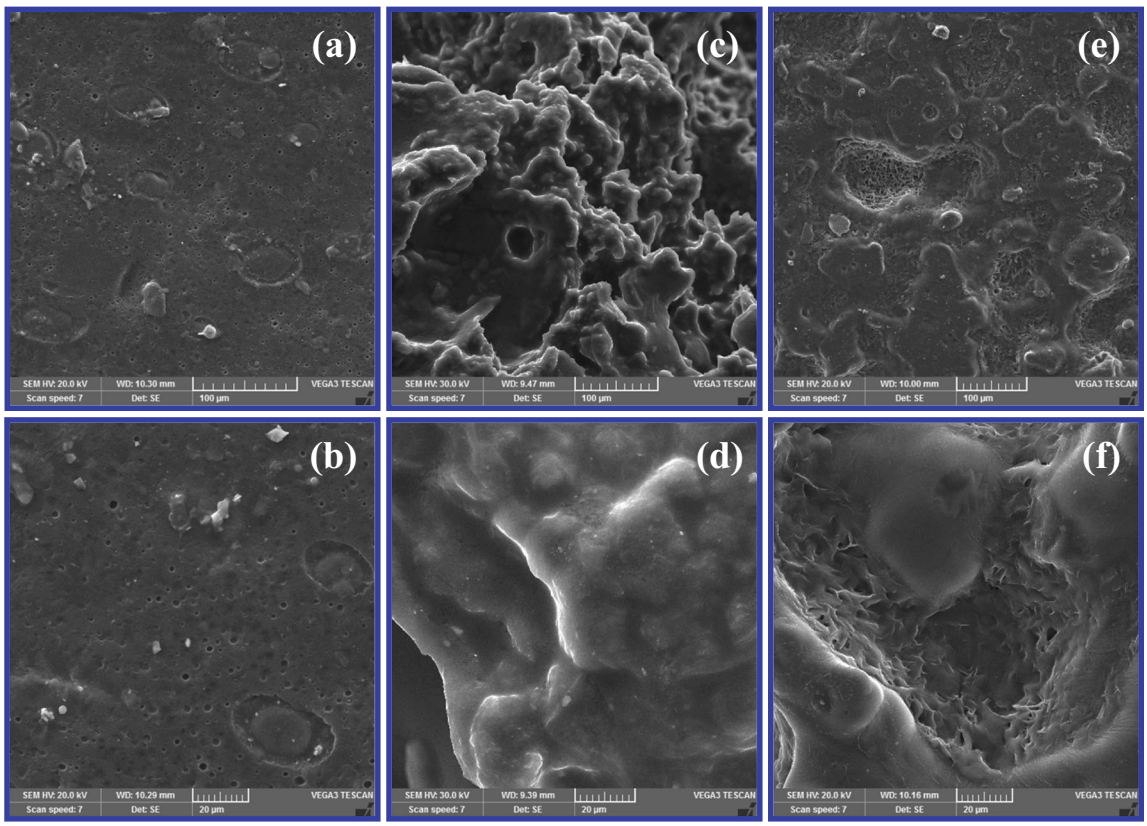

Fig. 3 SEM micrographs of (a, b) CS/GA/PEG, (c, d) BPEO-CS/GA/PEG, and (e, f) GEO-CS/GA/PEG composite films with different magnifications

PEG film. Similarly, Li et al. [14] reported that the encapsulation of turmeric EO into CS films increased the heterogeneity and roughness of the CS films; likewise, Abdollahi et al. [52] also reported a similar behavior when summer savory essential oil was encapsulated in carboxymethyl cellulose-agar biocomposite film.

3.2.8 Differential scanning calorimetry studies

Thermal properties of the CS/GA/PEG, BPEO-CS/GA/PEG, and GEO-CS/GA/PEG films measured by DSC are presented in Fig. 4. Two endothermic peaks were observed in the CS/GA/PEG composite film at 120 °C and 284 °C, which are mainly due to the evaporation of free water and degradation of film containing macromolecules such as CS, GA, and PEG (Fig. 4 (a)). A new endothermic peak appeared at 44 °C and 45 °C in the BPEO- (Fig. 4 (b)) and GEO- (Fig. 4 (c)) incorporated CS/GA/PEG composite films, respectively, which reveals the evaporation of EO components due to the weak molecular interaction between the both EOs with CS/GA/PEG composite matrix. The second endothermic peaks were observed at 98 °C (Fig. 4 (b)) and 91 °C (Fig. 4 (c)) for BPEO-CS/GA/PEG and GEO-CS/GA/PEG composite films, which are due to the evaporation of free water and residual moisture content [45, 53]. The third endothermic peaks were observed at 251 °C and 233 °C for BPEO- (Fig. 4 (b)) and GEO- (Fig. 4 (c)) incorporated CS/GA/PEG composite films, respectively, which was ascribed to the degradation of the film matrixes or the melting temperature of CS, GA, and PEG [34, 48, 54]. These observations indicated that the BPEO- and GEO-incorporated CS/GA/PEG films had relatively better molecular interaction with CS/GA/PEG matrix with good water resisting ability and retained occupancy residual water.

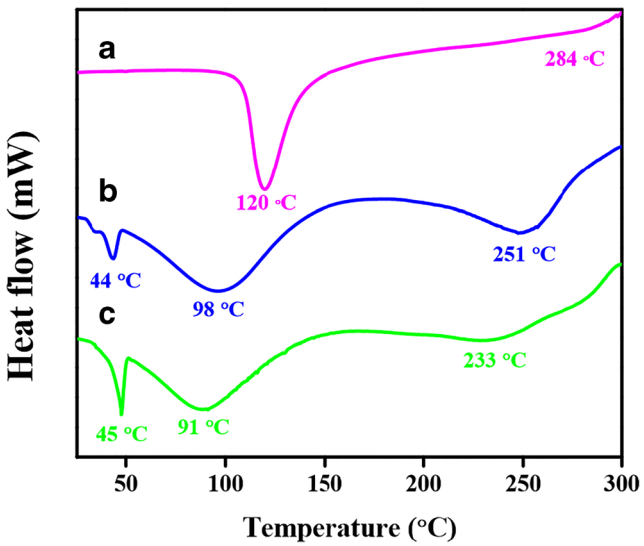

Fig. 4 DSC thermogram of (a) CS/GA/PEG, (b) BPEO-CS/GA/PEG, and (c) GEO-CS/GA/PEG composite films

3.3 Retention and release study

EOs are volatile and could suffer a great loss during the evaporation of film formation and subsequent storage. Both EOs, BPEO and GEO, in CS/GA/PEG composite films have shown significant retention during ambient storage, which is shown in Fig. 5A. The results indicated that the GEO had much higher retention than the BPEO from the CS/GA/PEG composite matrix that might be due to the chemical interactions between the EOs and composite matrix. Similar results were observed when incorporating soy bean oil and cinnamon bark oil encapsulated in CS film [55] and cinnamon EO in CS and GA based film [13].

The release study of both BPEO and GEO from the EO-incorporated CS/GA/PEG composite films was carried out for 48 h at pH 7. The release rate of both BPEO and GEO is divided into two stages based on the release rate (Fig. 5B). The initial burst release was observed for the first 12 h, both EOs, BPEO and GEO, were released up to 80.2% and 78.5%, respectively (Fig. 5B (insert)), due to the rapid discharge of EOs from the thin matrix of composite films. The second stage showed a slow release till 48 h where both BPEO and GEO were released up to 85.9% and 82.9%, respectively, (Fig. 5B) due to the migration of EOs from the deep matrix of film to the surface, because BPEO as well as GEO was connected and implanted in the cross-linking network structure of the film matrix made by CS, GA, and PEG. When the films were immersed in hexane solution, a really fast release of both BPEO and GEO happened at the initial contact time, and latterly the release rate of both EOs decreased during the rest of the period, which could be attributed to the easy and fast penetration of hexane into the composite film matrixes. The diffusion of EOs is also favored through the composite film matrix due to the swelling process, producing a more open structure and consequently increasing the EOs mobility [55, 56].

3.4 Antimicrobial study

The prepared CS/GA/PEG composite film showed a slight antibacterial activity against all tested organisms, which is likely due to the presence of CS [48] and GA [34]. Both BPEO- and GEO-incorporated CS/GA/PEG composite films showed a significant ($p < 0.05$) increase in the antibacterial activity, when compared with CS/GA/PEG composite film (Table 3). Among the EO-incorporated CS/GA/PEG composite films, GEO-CS/GA/PEG composite film showed a significant ($p < 0.05$) highest inhibition zone (16.58 ± 2.36 mm, 14.12 ± 1.36 mm, 13.14 ± 1.39 mm, and 14.17 ± 1.48 mm for *B. cereus*, *S. aureus*, *E. coli*, and *S. typhimurium*, respectively) among the composite films; however, BPEO-CS/GA/PEG composite film also registered significant inhibition zones (14.81 ± 1.85 mm, 11.49 ± 1.61 mm, 10.92 ± 1.49 mm, and 11.82 ± 1.66 mm for *B. cereus*, *S. aureus*, *E. coli*, and *S. typhimurium*, respectively).

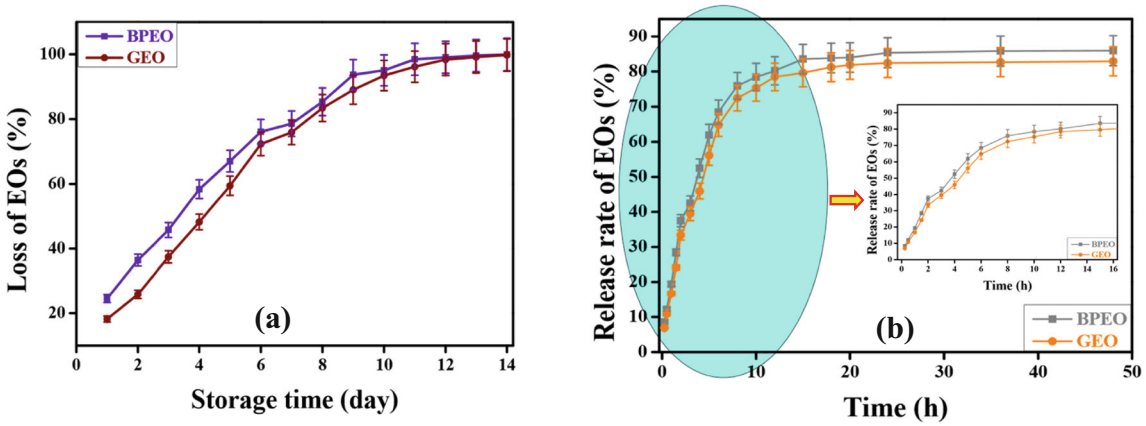

Fig. 5 (A) Loss of BPEO and GEO from the incorporated CS/GA/PEG composite films and (B) Release profile of BPEO and GEO from the incorporated CS/GA/PEG composite films (insert: initial burst release profile of BPEO and GEO)

The increasing effect of antibacterial activity also demonstrates that the incorporation of GEO and BPEO onto the CS/GA/PEG composite film is an efficient method for protecting and increasing the stability and sustains the release of their bioactive compounds. The sustained release of the EO molecules allows their continuous availability and destruction to the cytoplasmic membrane [13, 57, 58]. The results also indicated that a representative for gram-positive bacteria *B. cereus* and *S. aureus* was more sensitive to the tested composite films than the gram-negative bacteria composed of lipopolysaccharides and proteins that better tolerates the tested composite films containing GEO and BPEO. Moreover, the O-side chain of the lipopolysaccharide of the gram-negative bacteria has hydrophobic molecules to enter the bilayer [29, 59]. These results were also confirmed by the earlier studies, such as Sayyad et al. [60] and Noori et al. [11], and were reported that the antibacterial activity of EOs against gram positive is drastically higher than gram-negative bacteria. Likewise, in our earlier study, both EOs, BPEO and GEO, were well incorporated onto a polyvinyl alcohol/GA/CS composite film that have also confirmed their promising potential as an alternative of wound dressing and food packaging materials [61].

4 Conclusion

In this study, BPEO- and GEO-incorporated CS/GA/PEG composite films were successfully prepared by the solvent casting method, which could be a good alternative for the traditional food packaging and wound healing materials. The GEO-CS/GA/PEG nanocomposite film showed a hetero-structure with entrapment of GEO droplets with increased roughness and the appearance of more cavities without cracks due to the hydrophobicity of GEO, whereas the surface of the CS/GA/PEG composite film containing BPEO was rough surface with increased coarseness due to the migration of oil droplets towards the film surface. The BPEO- and GEO-incorporated CS/GA/PEG composite films showed high tensile strength and flexible nature with high heat stability. Both EO-incorporated CS/GA/PEG composite films were registered with good retention and release rate of respective EO, among them GEO-CS/GA/PEG composite film showed much better retention and release rate than the BPEO-CS/GA/PEG composite film. The BPEO- and GEO-incorporated CS/GA/PEG composite films were significantly inhibited the growth of *B. cereus*, *S. aureus*, *E. coli*, and *S. typhimurium*. The obtained results have demonstrated that both BPEO- and GEO-

Table 3 Antimicrobial activities of CS/GA/PEG composite films with and without BPEO and GEO

Composite film	Inhibition zone diameter (mm)			
	B. cereus	*S. aureus*	*E. coli*	*S. typhimurium*
CS/GA/PEG	5.74 ± 1.46	4.86 ± 1.27	3.89 ± 1.46	4.16 ± 1.28
BPEO-CS/GA/PEG	14.81 ± 1.85*	11.49 ± 1.61*	10.92 ± 1.49*	11.82 ± 1.66*
GEO-CS/GA/PEG	16.58 ± 2.36*	14.12 ± 1.36*	13.14 ± 1.39*	14.17 ± 1.48*

Values are mean ± SD of five replicates

Significant difference exists at $*p < 0.05$

incorporated CS/GA/PEG composite films are promising alternatives to food packaging and wound dressing materials.

Acknowledgments The authors would like to thank the management of Plant Lipids Private Ltd., Cochin, India, for their support and encouragement. We also wish to express our gratitude to our laboratory members for their active help and cooperation.

Compliance with ethical standards

Conflict of interest Three of the authors (A.A., K.K.J.R., and S.G.) are employees of Aurea Biolabs (P) Ltd., a research subsidiary of Plant Lipids Ltd. All other authors have no conflicts to report.

References

1. Silva FT, Cunha KF, Fonseca LM, Antunes MD, Halal SLME, Fiorentini ÂM, Zavareze ER, Dias ARG (2018) Action of ginger essential oil (Zingiber officinale) encapsulated in proteins ultrafine fibers on the antimicrobial control in situ. Int J Biol Macromol 118: 107–115
2. Hu J, Zhang Y, Xiao Z, Wang X (2018) Preparation and properties of cinnamon-thyme-ginger composite essential oil nanocapsules. Ind Crop Prod 122:85–92
3. Dima C, Pătrașcu L, Cantaragiu A, Alexe P, Dima Ş (2016) The kinetics of the swelling process and the release mechanisms of *Coriandrum sativum* L. essential oil from chitosan/alginate/inulin microcapsules. Food Chem 195:39–48
4. Chen S, Liu B, Carlson MA, Gombart A, Reilly D, Xie J (2017) Recent advances in electrospun nanofibers for wound healing. Nanomedicine 12:1335–1352
5. Ardekani NT, Khorram M, Zomorodian K, Yazdanpanah S, Veisi H, Veisi H (2019) Evaluation of electrospun poly (vinyl alcohol)-based nanofiber mats incorporated with Zataria multiflora essential oil as potential wound dressing. Int J Biol Macromol 125:743–750
6. Chen C, Xu Z, Ma Y, Liu J, Zhang Q, Tang Z, Fu K, Yang F, Xie J (2018) Properties, vapour-phase antimicrobial and antioxidant activities of active poly(vinyl alcohol) packaging films incorporated with clove oil. Food Control 88:105–112
7. Tang Y, Zhou Y, Lan X, Huang D, Luo T, Ji J, Mafang Z, Miao X, Wang H, Wang W (2019) Electrospun gelatin nanofibers encapsulated with peppermint and chamomile essential oils as potential edible packaging. J Agric Food Chem 67:2227–2234
8. Froiio F, Mosaddik A, Morshed MT, Paolino D, Fessi H, Elaissari A (2019) Edible polymers for essential oils encapsulation: application in food preservation. Ind Eng Chem Res 58:20932–20945
9. Xu L, Chu Z, Wang H, Cai L, Tu Z, Liu H, Zhu C, Shi H, Pan D-H, Pan J, Fei X (2019) Electrostatically assembled multilayered films of biopolymer enhanced nanocapsules for on-demand drug release. ACS Appl Bio Mater 2:3429–3438
10. Simon-Brown K, Solval KM, Chotiko A, Alfaro L, Reyes V, Liu C, Dzandu B, Kyereh E, Barnaby AG, Thompson I, Xu Z, Sathivel S (2016) Microencapsulation of ginger (Zingiber officinale) extract by spray drying technology. LWT - Food Sci Technol 70:119–125
11. Noori S, Zeynali F, Almasi H (2018) Antimicrobial and antioxidant efficiency of nanoemulsion-based edible coating containing ginger (Zingiber officinale) essential oil and its effect on safety and quality attributes of chicken breast fillets. Food Control 84:312–320
12. Matshetshe KI, Parani S, Manki SM, Oluwafemi OS (2018) Preparation, characterization and in vitro release study of β-cyclodextrin/chitosan nanoparticles loaded Cinnamomum zeylanicum essential oil. Int J Biol Macromol 118:676–682
13. Xu T, Gao CC, Yang Y, Shen X, Huang M, Liu S, Tang X (2018) Retention and release properties of cinnamon essential oil in antimicrobial films based on chitosan and gum arabic. Food Hydrocoll 84:84–92
14. Li Z, Lin S, An S, Liu L, Hu Y, Wan L (2019) Preparation, characterization and anti-aflatoxigenic activity of chitosan packaging films incorporated with turmeric essential oil. Int J Biol Macromol 131:420–434
15. Bonilla J, Vargas M, Atarés L, Chiralt A (2014) Effect of chitosan essential oil films on the storage-keeping quality of pork meat products. Food Bioprocess Technol 7:2443–2450
16. Shojaee-Aliabadi S, Hosseini H, Mohammadifar MA, Mohammadi A, Ghasemlou M, Hosseini SM, Khaksar R (2014) Characterization of kappa-carrageenan films incorporated plant essential oils with improved antimicrobial activity. Carbohydr Polym 101:582–591
17. Mayachiew P, Devahastin S, Mackey BM, Niranjan K (2010) Effects of drying methods and conditions on antimicrobial activity of edible chitosan films enriched with galangal extract. Food Res Int 43:125–132
18. Chen H, Hu X, Chen E, Wu S, McClements DJ, Liu S, Li B, Li Y (2016) Preparation, characterization, and properties of chitosan films with cinnamaldehyde nanoemulsions. Food Hydrocoll 61: 662–671
19. Peng H, Xiong H, Li J, Chen L, Zhao Q (2010) Methoxy poly(ethylene glycol)-grafted-chitosan based microcapsules: synthesis, characterization and properties as a potential hydrophilic wall material for stabilization and controlled release of algal oil. J Food Eng 101:113–119
20. Sánchez-González L, Cháfer M, Hernández M, Chiralt A, González-Martínez C (2011) Antimicrobial activity of polysaccharide films containing essential oils. Food Control 22:1302–1310
21. Hromiš NM, Lazić VL, Markov SL, Vaštag ŽG, Popović SZ, Šuput DZ, Džinić NR, Velićanski AS, Popović LM (2015) Optimization of chitosan biofilm properties by addition of caraway essential oil and beeswax. J Food Eng 158:86–93
22. Perdones Á, Chiralt A, Vargas M (2016) Properties of film-forming dispersions and films based on chitosan containing basil or thyme essential oil. Food Hydrocoll 57:271–279
23. Campelo PH, Junqueira LA, Resende JVD, Zacarias RD, Fernandes RVDB, Botrel DA, Borges SV (2017) Stability of lime essential oil emulsion prepared using biopolymers and ultrasound treatment. Int J Food Prop 20:S564–S579
24. Ozturk B, Argin S, Ozilgen M, McClements DJ (2015) Formation and stabilization of nanoemulsion-based vitamin E delivery systems using natural biopolymers: whey protein isolate and gum arabic. Food Chem 188:256–263
25. Krishnadev P, Gunasekaran K (2017) Development of gum arabic edible coating formulation through nanotechnological approaches and their effect on physicochemical change in tomato (Solanum lycopersicum L) fruit during storage. Int J Agric Sci 9:3866–3870
26. Mousa RMA (2018) Simultaneous inhibition of acrylamide and oil uptake in deep fat fried potato strips using gum arabic-based coating incorporated with antioxidants extracted from spices. Food Hydrocoll 83:265–274
27. Masood N, Ahmed R, Tariq M, Ahmed Z, Masoud MS, Ali I, Asghar R, Andleeb A, Hasan A (2019) Silver nanoparticle impregnated chitosan-PEG hydrogel enhances wound healing in diabetes induced rabbits. Int J Pharm 559:23–36
28. Mishra D, Khare P, Singh DK, Luqman S, Kumar PVA, Yadav A, Das T, Saikia BK (2018) Retention of antibacterial and antioxidant properties of lemongrass oil loaded on cellulose nanofibre-poly ethylene glycol composite. Ind Crop Prod 114:68–80
29. Rakmai J, Cheirsilp B, Mejuto JC, Torrado-Agrasar A, Simal-Gandara J (2017) Physico-chemical characterization and evaluation of bio-efficacies of black pepper essential oil encapsulated in hydroxypropyl-betacyclodextrin. Food Hydrocoll 65:157–164

30. Singh G, Maurya S, Catalan C, de Lampasona MP (2005) Studies on essential oils, part 42: chemical, antifungal, antioxidant and sprout suppressant studies on ginger essential oil and its oleoresin. Flavour Fragr J 20:1–6
31. Menon AN, Padmakumari KP, Jayalekshmy A (2003) Essential oil composition of four major cultivars of black pepper (Piper nigrum L.) III. J Essent Oil Res 15:155–157
32. Akyuz L, Kaya M, Ilk S, Cakmak YS, Salaberria AM, Labidi J, Yılmaz BA, Sargin I (2018) Effect of different animal fat and plant oil additives on physicochemical, mechanical, antimicrobial and antioxidant properties of chitosan films. Int J Biol Macromol 111:475–484
33. American Society for Testing and Materials (ASTM) (1995) Standard test methods of water vapor trans-mission of materials. Annual book of ASTM standards. American Society for Testing and Materials, Philadelphia, pp 96–95
34. Gopi S, Amalraj A, Kalarikkal N, Zhang J, Thomas S, Guo Q (2019) Preparation and characterization of nanocomposite films based on gum arabic, maltodextrin and polyethylene glycol reinforced with turmeric nanofiber isolated from turmeric spent. Mater Sci Eng C 97:723–729
35. Rouatbi M, Duquenoy A, Giampaoli P (2007) Extraction of the essential oil of thyme and black pepper by superheated steam. J Food Eng 78:708–714
36. Myszka K, Schmidt MT, Majcher M, Juzwa W, Czaczyk K (2017) β-Caryophyllene-rich pepper essential oils suppress spoilage activity of Pseudomonas fluorescens KM06 in fresh-cut lettuce. LWT - Food Sci Technol 83:118–126
37. Wang Y, Li R, Jiang Z-T, Tan J, Tang S-H, Li T-T, Liang L-L, He H-J, Liu Y-M, Li J-T, Zhang X-C (2018) Green and solvent-free simultaneous ultrasonic-microwave assisted extraction of essential oil from white and black peppers. Ind Crop Prod 114:164–172
38. Lia Y-X, Zhang C, Pan S, Chen L, Liu M, Yang K, Zeng X, Tian J (2020) Analysis of chemical components and biological activities of essential oils from black and white pepper (Piper nigrum L.) in five provinces of southern China. LWT - Food Sci Technol 117:108644
39. Hopkins EJ, Chang C, Lam RSH, Nickerson MT (2015) Effects of flaxseed oil concentration on the performance of a soy protein isolate-based emulsion-type film. Food Res Int 67:418–425
40. dos Santos Caetano K, Hessel CT, Tondo EC, Flôres SH, Cladera-Olivera F (2017) Application of active cassava starch films incorporated with oregano essential oil and pumpkin residue extract on ground beef. J Food Saf 37:e12355
41. Evangelho JA, Dannenberg GS, Biduski B, Halal SLM, Kringel DH, Gularte MA, Fiorentini AM, Zavareze ER (2019) Antibacterial activity, optical, mechanical, and barrier properties of corn starch films containing orange essential oil. Carbohydr Polym 222:114981
42. Sahraee S, Milani JM, Ghanbarzadeh B, Hamishehkar H (2017) Effect of corn oil on physical, thermal, and antifungal properties of gelatin-based nanocomposite films containing nano chitin. LWT-Food Sci Technol 76:33–39
43. Luís Â, Pereira L, Domingues F, Ramos A (2019) Development of a carboxymethyl xylan film containing licorice essential oil with antioxidant properties to inhibit the growth of foodborne pathogens. LWT - Food Sci Technol 111:218–225
44. Fabra MJ, Talens P, Chiralt A (2008) Tensile properties and water vapor permeability of sodium caseinate films containing oleic acid-beeswax mixtures. J Food Eng 85:393–400
45. Xue F, Gu Y, Wang Y, Li C, Adhikari B (2019) Encapsulation of essential oil in emulsion based edible films prepared by soy protein isolate-gum acacia conjugates. Food Hydrocoll 96:178–189
46. Fernandes RVB, Botrel DA, Silva EK, Borges SV, Oliveira CR, Yoshida MI, Feitosa JPA, de Paula RCM (2016) Cashew gum and inulin: new alternative for ginger essential oil microencapsulation. Carbohydr Polym 153:133–142
47. Rajeswari A, Amalraj A, Pius A (2015) Removal of phosphate using chitosan-polymer composites. J Environ Chem Eng 3:2331–2341
48. Gopi S, Amalraj A, Jude S, Thomas S, Guo Q (2019) Bionanocomposite films based on potato, tapioca starch and chitosan reinforced with cellulose nanofiber isolated from turmeric spent. J Taiwan Inst Chem Eng 96:664–671
49. Rajeswari A, Amalraj A, Pius A (2016) Adsorption studies for the removal of nitrate using chitosan/PEG and chitosan/PVA polymer composites. J Water Process Eng 9:123–134
50. Woranuch S, Yoksan R (2013) Eugenol-loaded chitosan nanoparticles: I. Thermal stability improvement of eugenol through encapsulation. Carbohydr Polym 96:578–585
51. Acevedo-Fani A, Salvia-Trujillo L, Martín-Belloso O (2015) Edible films from essential- oil-loaded nanoemulsions: physicochemical characterization and antimicrobial properties. Food Hydrocoll 47:168–177
52. Abdollahi M, Damirchi S, Shafafi M, Rezaei M, Ariaii P (2019) Carboxymethyl cellulose-agar biocomposite film activated with summer savory essential oil as an antimicrobial agent. Int J Biol Macromol 126:561–568
53. Gheribi R, Puchot L, Verge P, Jaoued-Grayaa N, Mezni M, Habibi Y, Khwaldia K (2018) Development of plasticized edible films from opuntia ficus-indica mucilage: a comparative study of various polyol plasticizers. Carbohydr Polym 190:204–211
54. Şentürk SB, Kahraman D, Alkan C, Gökçe İ (2011) Biodegradable PEG/cellulose, PEG/agarose and PEG/chitosan blends as shape stabilized phase change materials for latent heat energy storage. Carbohydr Polym 84:141–144
55. Ma Q, Zhang Y, Critzer F, Davidson PM, Zivanovic S, Zhong Q (2016) Physical, mechanical, and antimicrobial properties of chitosan films with microemulsions of cinnamon bark oil and soybean oil. Food Hydrocoll 52:533–542
56. Fernandez-Pan I, Mate JI, Gardrat C, Coma V (2015) Effect of chitosan molecular weight on the antimicrobial activity and release rate of carvacrol-enriched films. Food Hydrocoll 51:60–68
57. Nostro A, Scaffaro R, D'Arrigo M, Botta L, Filocamo A, Marino A, Bisignano G (2012) Study on carvacrol and cinnamaldehyde polymeric films: mechanical properties, release kinetics and antibacterial and antibiofilm activities. Appl Microbiol Biotechnol 96:1029–1038
58. Zhang Y, Liu X, Wang Y, Jiang P, Quek S (2016) Antibacterial activity and mechanism of cinnamon essential oil against Escherichia coli and Staphylococcus aureus. Food Control 59: 282–289
59. Zengin H, Baysal AH (2014) Antibacterial and antioxidant activity of essential oil terpenes against pathogenic and spoilage-forming bacteria and cell structure-activity relationships evaluated by SEM microscopy. Molecules 19:17773–17798
60. Sayyad SF, Chaudhari SR (2010) Isolation of volatile oil from some plants of Zingiberaceae family and estimation of their antibacterial potential. J Curr Pharm Res 4:1–3
61. Amalraj A, Haponiuk JT, Thomas S, Gopi S (2020) Preparation, characterization and antimicrobial activity of polyvinyl alcohol/gum arabic/chitosan composite films incorporated with black pepper essential oil and ginger essential oil. Int J Biol Macromol 151: 366–375